

Bioconversion Variation of Ginsenoside CK Mediated by Human Gut Microbiota From Healthy Volunteers and Colorectal Cancer Patients

Yin-Ping Guo

Central South University

Li Shao

Hunan University of Chinese Medicine

Li Wang

Central South University

Man-Yun Chen

Central South University

Wei Zhang

Central South University

Wei-Hua Huang (✉ endeavor34852@aliyun.com)

Central South University

Research

Keywords: Ginsenoside CK, gut microbiota, LC-MS/MS, colorectal cancer, 16S rRNA gene sequencing

Posted Date: February 5th, 2021

DOI: <https://doi.org/10.21203/rs.3.rs-181900/v1>

License: © ⓘ This work is licensed under a Creative Commons Attribution 4.0 International License.

[Read Full License](#)

Version of Record: A version of this preprint was published on March 17th, 2021. See the published version at <https://doi.org/10.1186/s13020-021-00436-z>.

Abstract

Background: Ginsenoside CK (GCK) serves as the potential anti-colorectal cancer (CRC) protopanaxadiol (PPD)-type saponin, which could be mainly bio-converted to yield PPD by gut microbiota. Meanwhile, the anti-CRC effects of GCK could be altered by gut microbiota due to its different diversity in CRC patients. We aimed to investigate the bioconversion variation of GCK mediated by gut microbiota from CRC patients by comparing with healthy subjects.

Methods: Gut microbiota profiled by 16S rRNA gene sequencing was collected from healthy volunteers and CRC patients. GCK was incubated with gut microbiota *in vitro*. A LC-MS/MS method was validated to quantify GCK and PPD after incubation at different time points.

Results: The bioconversion of GCK in healthy subjects group was much faster than CRC group, as well as the yield of PPD. Moreover, significant difference of PPD concentration between healthy subjects group and CRC group could be observed at 12 h, 48 h and 72 h check points. According to 16S rRNA sequencing, the profiles of gut microbiota derived from healthy volunteers and CRC patients significantly varied, in which 12 differentially abundant taxon were found, such as *Bifidobacterium*, *Roseburia*, *Bacteroides* and *Collinsella*. Spearman's correlation analysis showed bacteria enriched in healthy subjects group were positively associated with biotransformation of GCK, while bacteria enriched in CRC group displayed non correlation characters. Among them, *Roseburia* which could secrete β -glycosidase showed the strongest positive association with the bioconversion of GCK.

Conclusion: The bioconversion of GCK in healthy subjects was much faster than CRC patients mediated by gut microbiota, which might alter the anti-CRC effects of GCK.

Introduction

Ginsenoside CK (GCK) is one of the most abundant metabolites of protopanaxadiol (PPD)-type saponins bio-converted by gut microbiota in the intestinal tract, which is the major adsorption plasma substance of PPD-type saponins into circulatory system [1, 2]. GCK exhibits various pharmacological properties, i.e., anti-colorectal cancer (CRC) and anti-inflammation [3, 4]. Interestingly, GCK shows stronger anti-CRC effects than its parent ginsenosides, such as ginsenoside Rb₁, Rc and Rd [5, 6]. Meanwhile, GCK could be metabolized by gut microbiota to generate the aglycon PPD, which could also be determined in plasma after oral administration of GCK at any dosage in phase I clinical trial [7, 8]. The pertinent results have indicated that GCK could be delivered into intestinal tract and further metabolized by gut microbiota [9]. The data imply that the bioconversion of GCK mediated by gut microbiota could lead to different responses on its anti-CRC effects.

Gut microbiota could be modulated by many factors linked to physiologic health and disease including CRC [10, 11]. The profile of gut microbiota is significantly different between CRC patients and healthy volunteers [12, 13]. For example, *Bifidobacterium* and *Lactobacillus* are significantly higher in the healthy volunteers than CRC patients, while healthy volunteers possess a relative lower abundance of

Bacteroides. Herein, the bioconversion of GCK might be very different due to the variation of gut microbiota between healthy subjects and CRC patients, which could alter the anti-CRC effects of GCK. Therefore, it is meaningful to investigate the bioconversion of GCK mediated by gut microbiota derived from CRC patients and healthy volunteers.

In this study, GCK and PPD were quantified by a validated LC-MS/MS method after *in vitro* incubation with gut microbiota at different time point. Gut microbiota collected from CRC patients and healthy volunteers was profiled by 16S rRNA gene sequencing. The results demonstrated that the bioconversion of GCK mediated by gut microbiota derived from healthy subjects was much faster than CRC patients.

Materials And Methods

Chemical and materials

The standard 20(*S*)-GCK and 20(*S*)-protopanaxatriol (PPT) were purchased from Chengdu Push Biotechnology Co., Ltd (Sichuan, China), and 20(*S*)-PPD was supplied by Baoji Herbest Bio-Tech Co., Ltd (Shaanxi, China). Their chemical structures were presented in Fig. 1. Acetonitrile (ACN) and methanol in HPLC-grade were obtained from Merck Company (Darmstadt, Germany).

Fecal samples preparation

The stool samples were collected from 11 CRC patients (CRC group) and 11 healthy volunteers (health group), respectively, who had not taken any probiotics or antibiotics in the last 30 days and abused alcohol or tobacco. CRC patients were screened and diagnosed through physical examination, who had similar body-mass index value with healthy volunteers (22.69 ± 1.69 for CRC group, and 21.58 ± 1.72 for health group). Gut microbiota was prepared from fresh fecal samples immediately, while the remained samples were stored in a $-80\text{ }^{\circ}\text{C}$ freezer until sequencing.

Biotransformation of GCK

Fresh fecal samples (1 g) were suspended in 15 mL of cold sterile physiological saline by following the preparation process described in our previous work [9]. The stocks of gut microbiota suspension were cultured with 10 fold volume of general anaerobic medium (GAM) broth in an E500 anaerobic chamber (Gene Science, USA) at $37\text{ }^{\circ}\text{C}$ for activation. After incubation for 24 h, the suspension was centrifuged at 4000 rpm for 20 min at $4\text{ }^{\circ}\text{C}$, and then 5 mL of GAM broth were used to re-suspend the precipitate as work solution of gut microbiota.

The biotransformation of GCK mediated by gut microbiota *in vitro* was performed in 0.5 mL of incubation system, which contained 2.5 μL of GCK solution (dissolved in DMSO, 50 $\mu\text{g}/\text{mL}$), 100 μL of work solution of gut microbiota and 398 μL of GAM broth. The incubation system was incubated at 37°C in the anaerobic chamber (80% N_2 , 10% H_2 and 10% CO_2) for 1 h, 2 h, 4 h, 8 h, 12 h, 24 h, 48 h and 72 h. Samples were prepared in triplicate for each time check point.

Sample preparation

The incubation mixture was extracted with 0.5 mL of ethyl acetate and 0.5 mL of water saturated n-butanol by using a vortex for 10 min, respectively. The extracted supernatant was mixed together and dried under nitrogen at room temperature. The residues were re-dissolved with 100 μ L of methanol and then centrifuged at 13000 rpm for 10 min before analysis.

Instrumentation and analytical conditions

GCK and PPD were quantified in the negative ion mode on an AB SCIEX 6500+ Triple Quad LC-MS/MS system (AB SCIEX, UAS). The chromatographic separation was achieved on an ACQUITY BEH Shield RP18 column (Waters, USA, 50 \times 2.1 mm, 1.7 μ m) with a gradient elution of 2 mM ammonium acetate in water (A) and ACN (B) at a flow rate of 0.3 mL/min. The gradient profile was optimized as following, 20% (B) for 0.01 - 1 min, 20% - 65% (B) for 1 - 2 min, 65 - 75% (B) for 2 - 3 min, 75 - 90% (B) for 3 - 4 min, 90 - 100% (B) for 4 - 5 min and 100% (B) for 5 - 6 min. The mass spectrometer parameters were optimized as following, ion source gas 1 and 2, 45 psi (nitrogen); curtain gas, 25 psi (nitrogen); temperature, 450 $^{\circ}$ C and ion spray voltage, -4500V. The optimized MRM parameters of each compound were listed in Supplementary Table 1. The injection volume was 2 μ L, while the system was controlled by AB SCIEX Analyst TF software (version 1.6).

Calibration standards and quality control (QC) samples

The primary stock solutions of GCK (0.408 mg/mL), PPD (0.402 mg/mL) and PPT (IS, 0.196 mg/mL) were prepared by dissolving each compound in methanol, respectively. Working solutions were prepared by diluting the stock solutions appropriately with methanol-water (V: V = 1:1) and stored at 4 $^{\circ}$ C. The standard calibration curves samples and QC samples were prepared by spiking 2.5 μ L of working solution with 100 μ L of gut microbiota work solution and 398 μ L of GAM broth (blank gut microbiota medium). The solution of PPT (IS) was diluted to 1.96 μ g/mL using methanol-water.

Method validation

The method was validated by following respect to selectivity, sensitivity, linearity, precision, accuracy, recovery and matrix effect according to the United States Food and Drug Administration (FDA) guidelines. The selectivity of this method was evaluated by comparing chromatograms of extracted blank gut microbiota solution obtained from six different human feces samples with that spiked with GCK (0.51 μ g/mL), PPD (0.5025 μ g/mL) and PPT (1.96 μ g/mL) work solutions. The seven-point standard curves, ranging from 2.55 ng/mL to 408 ng/mL for GCK and 2.51 ng/mL to 402 ng/mL for PPD, were plotted on the peak area ratio of target ions to the IS versus the corresponding concentrations by a weighted ($1/X^2$) linear least squares regression model. The intra- and inter-day precision and accuracy were determined by analyzing six replicate samples at each QC level within one day and three consecutive days. The QC samples were set at 2.55 ng/mL, 7.65 ng/mL, 51 ng/mL and 306 ng/mL for GCK, and 2.51 ng/mL, 7.54

ng/mL, 50.25 ng/mL and 301.5 ng/mL for PPD. The recovery and matrix effect were investigated accordingly.

16S rRNA gene sequencing

Microbial genomic DNA was extracted from fecal samples by using Qiagen QIAamp DNA Stool Mini Kit (Qiagen, Germany), and the V3-V4 region of the bacteria 16S rRNA gene was amplified by PCR using primers 341F 5'-CCTAYGGGRBGCASCAG-3' and 806R 5'-GGACTACNNGGGTATCTAAT-3'. Amplicons were extracted and purified by using GeneJET Gel Extraction Kit (ThermoScientific, USA). Sequencing libraries were constructed by using Ion Plus Fragment Library Kit 48 rxns (ThermoFisher, USA). Purified amplicons were sequenced on Ion S5™XL platform (ThermoFisher, USA) according to the standard protocols.

Bioinformatics analysis

Bioinformatics analysis of bacteria 16S rRNA sequencing data was conducted by using QIIME 2 software [14] (version 2018.11, <https://qiime2.org>). Raw sequence data were developed into clean data by cut off the barcode and primer sequences (Cutadapt plugin), de-multiplexed (demux plugin), and denoised with DADA2 (Dada2 plugin) [15]. Operational Taxonomic Units (OTUs) were clustered with 97% similarity cutoff, and the GreenGene Database (<http://greengenes.lbl.gov/cgi-bin/nph-index.cgi>) was applied for the taxonomic classification. Alpha diversity and beta diversity were analyzed by Diversity plugin.

To analyze the alpha diversity, Shannon index was calculated to assess community diversity. Observed OTUs were used for evaluating the richness. Faith's index was applied to phylogenetic diversity, while Pielou's index was employed to estimate the evenness of communities. The data were visualized by using GraphPad Prism (version 7.00). Beta diversity was assessed by using principal co-ordinates analysis (PCoA). Bray Curtis distance and Jaccard distance were calculated according to phylogenetic measures, while Unweighted Unifrac distance and Weighted Unifrac distance were employed for the sequence measures. Moreover, the linear discriminative analysis effect size (LDA effect size, LEfSe) analysis was conducted to discover the differentially abundant taxon by using LEfSe software (LDA score >4). Furthermore, Phylogenetic Investigation of Communities by Reconstruction of Unobserved States (PICRUSt) analysis was used to predict the metabolic function of bacteria, of which the different function was expressed as LDA scores (LDA scores >2). Lastly, a heat map of Spearman's correlations was constructed by using gplots and RColorBrewer packages of R software (version 4.0.0).

Statistical analysis

Statistical analyses was performed on SPSS software (version 17.0), and significant differences were expressed as * $p < 0.05$, ** $p < 0.01$ and # $p < 0.001$.

Results

Method validation

A LC-MS/MS method was successfully validated for quantification of GCK and PPD in the incubation system. Representative MRM chromatograms of GCK, PPD, PPT and the corresponding blank gut microbiota solution were shown in SFig. 1. The developed method displayed a good selectivity for GCK and PPD. Supplementary Table 2 presented the validation data for linearity range, correlation coefficients (r), calibration curves and LLOQ of GCK and PPD. Both calibration curves showed good linearity ($r \geq 0.9987$), and the LLOQ was 2.55 ng/mL for GCK and 2.51 ng/mL for PPD. The results of precision and accuracy were listed in Supplementary Table 3. The intra- and inter-day precision was ranged from 1.8% to 7.2% for GCK and 2.1% to 9.8% for PPD, while the intra- and inter-day accuracy was ranged from 95.5% to 100.1% for GCK and 94.7% to 102.5% for PPD. Supplementary Table 4 showed the results of recovery and matrix effect. The recovery of GCK and PPD was ranged from 86.3% to 92.9% and 85.8% to 94.0%, respectively. The matrix effect of GCK and PPD were ranged from 4.6% to 8.3% and 6.7% to 8.9%, respectively, which indicated that no endogenous substances significantly suppressed or enhanced the ionization of both compounds, as well as the IS. Overall, the developed LC-MS/MS method was successfully validated to quantify GCK and PPD in gut microbiota incubation system.

Biotransformation of GCK

As shown in Table 1 and Fig. 2a-p, compared with CRC group, the concentration of GCK in the health group decreased rapidly during 0 h to 4 h. PPD could be initially detected at 1 h in the health group, but it could be determined at 4 h in the CRC group. Meanwhile, the concentration of PPD at 12 h, 48 h and 72 h in the health group was significantly higher than CRC group. Fig. 2q showed that the bioconversion rate of GCK in the health group was much higher than CRC group at all check-points. These results demonstrated bioconversion variation of GCK between health group and CRC group due to the different gut microbiota derived from healthy volunteers and CRC patients.

Table 1

Mean concentration of GCK and PPD in the incubation system at each time point

Time	Health Group (ng/mL)		CRC group (ng/mL)	
	GCK	PPD	GCK	PPD
0 h	150.26	0	137.82	0
1 h	141.50	0.74	136.54	0
2 h	113.33	2.48	135.62	0
4 h	86.99	9.85	127.88	0.98
8 h	79.08	19.48	104.60	4.90
12 h	76.90	26.57	97.75	5.85
24 h	73.94	34.80	84.43	15.87
48 h	59.70	47.06	86.93	18.05
72 h	56.06	50.90	77.28	21.51

Alpha and beta diversity of gut microbiota

As presented in Fig. 3a-d, Shannon index, Observed OTUs and Faith's index had higher levels in CRC group than health group, which implied a higher alpha diversity within microbial communities of CRC group. The results of beta diversity were presented in Fig. 3e-h, which showed that all samples could be clustered into two group unambiguously. The 16S rRNA sequencing data provided that the alpha and beta diversity of gut microbiota were significantly different between health group and CRC group.

Taxonomic differences of gut microbiota

Taxonomical classification was performed on five levels (phylum, class, order, family and genus). Fig. 4a-b showed the relative abundance of top five phylum level bacteria in two groups. Compared with CRC group, the relative abundance of *Firmicutes* was much higher in health group, while *Bacteroidetes* significantly decreased. Top ten bacteria of both groups in genus level were *Bacteroides*, *Faecalibacterium*, *Blautia*, *Roseburia*, *Bifidobacterium*, *Prevotella*, *Coprococcus*, *SMB53*, *Oscillospira* and *Ruminococcus*.

We also conducted LEfSe analysis as a tool to discover the differentially abundant taxon. In genus level, 12 bacteria ($p < 0.05$, LDA scores > 4) were found, which could be mainly categorized into *Actinobacteria*, *Firmicutes*, *Proteobacteria* and *Bacteroidetes* (Phylum), and their taxonomical information were listed in Supplementary Table 5. Fig. 4c-d showed that *Bifidobacterium*, *Blautia*, *Corynebacterium*, *Enhydrobacter*,

Faecalibacterium, *Roseburia*, *Rothia* and *SMB53* were enriched in health group, while *Bacteroides*, *Collinsella*, *Coprobacillus* and *Enterobacteriaceae* increased comparatively in CRC group. Among them, *Bacteroides*, *Bifidobacterium*, *Blautia*, *Faecalibacterium*, *Roseburia*, and *SMB53* were the predominant abundant bacteria in genus level (Fig. 4e-f and SFig. 2).

Lastly, the metabolic function of bacteria was predicted using PICRUSt analysis. A total of 328 KEGG pathways had been enriched, 41 functional pathways of which showed significant difference between health group and CRC group ($p < 0.05$, LDA scores > 2). The data (SFig. 3) showed that ABC transporters, sporulation, porphyrin and chlorophyll metabolism were obviously enriched in health group, while amino and nucleotides metabolism and lipopolysaccharide biosynthesis proteins were enriched in CRC group. These findings proved that the profiles of gut microbiota derived from CRC group were discriminated from health group.

Correlation between the biotransformation of GCK and gut microbiota

For better understanding the relationship of gut microbiota and bioconversion of GCK, Spearman's correlation index were calculated between the concentration of PPD, bioconversion rate of GCK and the relative abundance of 12 differentially abundant taxon (Fig. 5). Bacteria enriched in health group were positively correlated with the biotransformation of GCK, while bacteria enriched in CRC group showed non correlation characters. Among them, *Blautia*, *Enhydrobacter*, *Faecalibacterium* and *Roseburia* showed strong positive correlations with biotransformation rate of GCK and PPD, while *Coprobacillus* and *Enterobacteriaceae* were negatively correlated with them. In addition, *Roseburia* showed significant correlation with PPD yield after incubation at 1 h, 4 h, 8 h and 12 h, while the Spearman correlation provided the highest value (0.603) between its relative abundance and PPD yield at 4 h. The data implied that *Roseburia* might be a main contributor for the bioconversion variation of GCK between health group and CRC group.

Discussion

In our study, the bioconversion rate of GCK in the healthy volunteers was higher than CRC group, which implied that GCK and PPD absorbed into human plasma would be different between healthy and CRC patients after oral administration with equivalent dose of GCK. Similarly, *in vivo* effects after oral administration with GCK might be also varied. Moreover, PPD also showed different pharmaceutical activities, such as anti-inflammatory and anti-CRC effects [16]. However, anti-CRC effects of GCK pertinent to gut microbiota were still unknown.

In addition, besides genetic impacts, gut microbiota are also re-shaped by many environmental factors, such as gastro-intestinal diseases [17]. Hence, we recruited CRC patients from physical examination center without any drug treatments. Meanwhile, gut microbiota of CRC patients and healthy volunteers were profiled by 16S rRNA gene sequencing due to individual variation. The annotation results showed the ratio of *Firmicutes* phyla to *Bacteroidetes* phyla was lower in CRC subjects, which was consistent with the reported literatures, as well as some top ten gut microbials in genus level, such as *Bacteroides* and

Roseburia [12]. The results of LEfSe analysis found that *Bifidobacterium* and *Roseburia* were enriched in health group, while *Bacteroides* and *Collinsella* were enriched in CRC patients [12, 18]. These data indicated that profiles of gut microbiota derived from CRC and healthy subjects displayed significant differences.

In addition, the results of Spearman's correlation analysis found that 4 genus bacteria were positively associated with the bioconversion of GCK. As the metabolism of GCK was catalyzed by β -glycosidase, the ability of gut microbiota to secrete these key enzymes should also be predominantly considered. Studies verify that more than half of the low G + C% Gram-positive *Firmicutes* harbored β -glycosidase, as well as *bifidobacterium spp.* and *lactobacillus* [19, 20]. At the same time, *Bifidobacterium*, *Ruminococcus* and *Roseburia* could secrete β -glycosidase [20, 21]. Importantly, our previous work had also verified that PPD-type ginsenosides could be bio-converted by *Bacteroides ovatus*. Therefore, *Roseburia*, which belongs to butyrate-producing bacteria and alleviates experimental colitis pathology by inducing anti-inflammatory responses (such as *Roseburia intestinalis*) [22, 23], might play an essential role on the bioconversion variation of GCK between healthy subjects and CRC patients.

As gut microbiota provide crucial signals for development and function of host immune system, more and more studies reported that drugs have interaction with gut microbiota [17, 24]. In this study, we only focused on the bioconversion of GCK mediated by gut microbiota, but the effects of GCK on gut microbiota were not investigated, which might also play an important role on its biological activities.

Conclusion

A LC-MS/MS method was validated to quantify GCK and PPD in the gut microbiota incubation system. The bioconversion rate of GCK mediated by gut microbiota derived from healthy subjects was much higher than CRC patients. The profiles of gut microbiota between health subjects and CRC patients were significantly different through 16S rRNA sequencing. *Roseburia* might be a main contributor for bioconversion variation of GCK.

Abbreviations

ACN: acetonitrile; GCK: Ginsenoside CK; CRC: colorectal cancer; GAM: General anaerobic medium; LDA: the linear discriminative analysis; LEfSe: the linear discriminative analysis effect size; OTUs: Operational Taxonomic Units; PCoA: principal co-ordinates analysis; PICRUSt: Phylogenetic Investigation of Communities by Reconstruction of Unobserved States; PPD: protopanaxadiol; PPT: protopanaxatriol; QC: quality control.

Declarations

Ethics approval and consent to participate

These procedures involved feces samples collection were approved by Ethics Committee of Central South University.

Consent for publication

All participants signed informed consent.

Availability of data and materials

The research data generated from this study are included within the article and supplementary files.

Competing interests

The authors declare that they have no competing interests.

Funding

This work was supported by the National Natural Scientific Foundation of China (82074000, 81903784), the Hunan Provincial Natural Science Foundation of China (2020JJ4878), the Scientific Research Project of Department of Education of Hunan Province (20K136), and NHC Key Laboratory of Birth Defect for Research and Prevention (Hunan Provincial Maternal and Child Health Care Hospital, No. KF2020002).

Authors' contributions

WH designed the experiments; YG participated in the experiments and analyzed the 16S rRNA sequencing data; MC, LW, LS and WZ provided the technical support and advices for the study; YG and WH wrote the manuscript. All authors approved the final version of manuscript.

Acknowledgements

Not applicable.

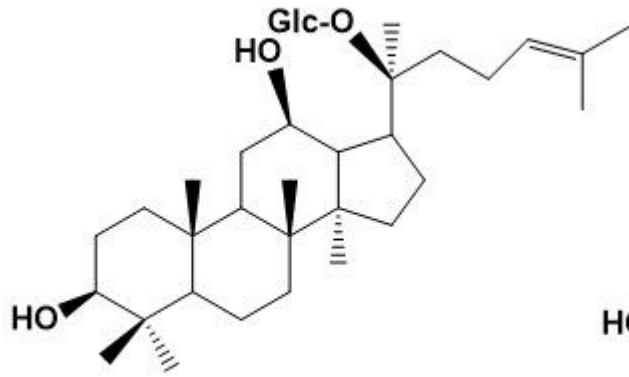
References

1. Yang X, Yang YY, Ouyang DS, Yang GP. A review of biotransformation and pharmacology of ginsenoside compound K. *Fitoterapia*. 2015;100:208-220.
2. Guo YP, Shao L, Chen MY, Qiao RF, Zhang W, Yuan JB, et al. In vivo metabolic profiles of Panax notoginseng saponins mediated by gut microbiota in rats. *J Agric Food Chem*. 2020;68(25):6835-6844.
3. Zhang Z, Du GJ, Wang CZ, Wen XD, Calway T, Li Z, et al. Compound K, a Ginsenoside Metabolite, Inhibits Colon Cancer Growth via Multiple Pathways Including p53-p21 Interactions. *Int J Mol Sci*. 2013;14(2):2980-2995.
4. Li J, Zhong W, Wang W, Hu S, Yuan J, Zhang B, et al. Ginsenoside Metabolite Compound K Promotes Recovery of Dextran Sulfate Sodium-Induced Colitis and Inhibits Inflammatory Responses by

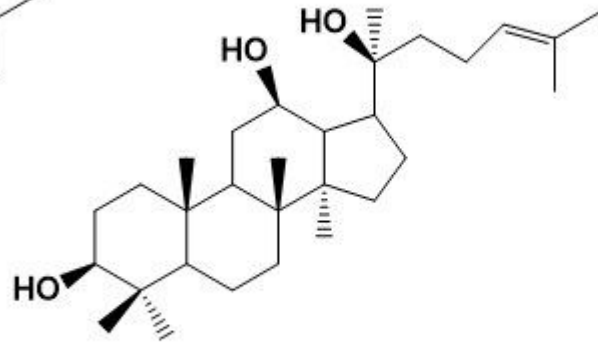
- Suppressing NF- κ B Activation. *PLoS One*. 2014;9(2):e87810
5. Wang CZ, Du GJ, Zhang Z, Wen XD, Calway T, Zhen Z, et al. Ginsenoside compound K, not Rb1, possesses potential chemopreventive activities in human colorectal cancer. *Int J Oncol*. 2012;40(6):1970-1976.
 6. Wang CZ, Cai Y, Anderson S, Yuan CS. Ginseng Metabolites on Cancer Chemoprevention: An Angiogenesis Link?. *Diseases*. 2015;3(3):193-204.
 7. Chen L, Zhou L, Huang J, Wang Y, Yang G, Tan Z, et al. Single- and Multiple-Dose Trials to Determine the Pharmacokinetics, Safety, Tolerability, and Sex Effect of Oral Ginsenoside Compound K in Healthy Chinese Volunteers. *Front Pharmacol*. 2018;8:965.
 8. Chen L, Zhou L, Wang Y, Yang G, Huang J, Tan Z, et al. Food and Sex-Related Impacts on the Pharmacokinetics of a Single-Dose of Ginsenoside Compound K in Healthy Subjects. *Front Pharmacol*. 2017;8:636.
 9. Chen MY, Shao L, Zhang W, Wang CZ, Zhou HH, Huang WH, et al. Metabolic analysis of Panax notoginseng saponins with gut microbiota-mediated biotransformation by HPLC-DAD-Q-TOF-MS/MS. *J Pharm Biomed Anal*. 2017;150: 199-207.
 10. Rinninella E, Raoul P, Cintoni M, Franceschi F, Miggiano GAD, Gasbarrini A, et al. What is the Healthy Gut Microbiota Composition? A Changing Ecosystem across Age, Environment, Diet, and Diseases. *Microorganisms*. 2019;7(1).
 11. Alvarez-Mercado AI, Navarro-Oliveros M, Robles-Sanchez C, Plaza-Diaz J, Saez-Lara MJ, Munoz-Quezada S, et al. Microbial Population Changes and Their Relationship with Human Health and Disease. *Microorganisms*. 2019;7(3).
 12. Wang T, Cai G, Qiu Y, Fei N, Zhang M, Pang X, et al. Structural segregation of gut microbiota between colorectal cancer patients and healthy volunteers. *ISME J*. 2012;6(2):320-329.
 13. Flemer B, Lynch DB, Brown JM, Jeffery IB, Ryan FJ, Claesson MJ, et al. Tumour-associated and non-tumour-associated microbiota in colorectal cancer. *Gut*. 2017;66(4):633-643.
 14. Bolyen E, Rideout JR, Dillon MR, Bokulich NA, Abnet CC, Al-Ghalith GA, et al. Reproducible, interactive, scalable and extensible microbiome data science using QIIME 2. *Nat Biotechnol*. 2019;37(8):852-857.
 15. Callahan BJ, McMurdie PJ, Rosen MJ, Han AW, Johnson AJ, Holmes SP. DADA2: High-resolution sample inference from Illumina amplicon data. *Nat Methods*. 2016;13(7):581-583.
 16. Wang M, Li H, Liu W, Cao H, Hu X, Gao X, et al. Dammarane-type leads panaxadiol and protopanaxadiol for drug discovery: Biological activity and structural modification. *Eur J Med Chem*. 2020;189:112087.
 17. Wu H, Esteve E, Tremaroli V, Khan MT, Caesar R, Manneras-Holm L, et al. Metformin alters the gut microbiome of individuals with treatment-naive type 2 diabetes, contributing to the therapeutic effects of the drug. *Nat Med*. 2017;23(7):850-858.
 18. Gueimonde M, Ouwehand A, Huhtinen H, Salminen E, Salminen S. Qualitative and quantitative analyses of the bifidobacterial microbiota in the colonic mucosa of patients with colorectal cancer,

- diverticulitis and inflammatory bowel disease. *World J Gastroentero.* 2007;13(29):3985-3989.
19. Yuksekdag Z, Acar BC, Aslim B, Tukenmez U. β -Glucosidase activity and bioconversion of isoflavone glycosides to aglycones by potential probiotic bacteria. *Int J Food Prop.* 2018;20(sup3):S2878-S2886.
 20. Dabek M, Mccrae SI, Stevens VJ, Duncan SH, Louis P. Distribution of beta-glucosidase and beta-glucuronidase activity and of beta-glucuronidase gene gus in human colonic bacteria. *FEMS Microbiol Ecol.* 2008;66(3):487-95.
 21. Avila M, Hidalgo M, Sánchez-Moreno C, Pelaez C, Requena T, Pascual-Teresa Sd. Bioconversion of anthocyanin glycosides by Bifidobacteria and Lactobacillus. *Food Res Int.* 2009;42(10):1453-1461.
 22. Marchesi JR, Adams DH, Fava F, Hermes GD, Hirschfield GM, Hold G, et al. The gut microbiota and host health: a new clinical frontier. *Gut.* 2016;65(2):330-9.
 23. Shen Z, Zhu C, Quan Y, Yang J, Yuan W, Yang Z, et al. Insights into Roseburia intestinalis which alleviates experimental colitis pathology by inducing anti-inflammatory responses. *J Gastroen Hepatol.* 2018;33(10):1751-1760.
 24. Rooks MG, Garrett WS. Gut microbiota, metabolites and host immunity. *Nat Rev Immunol.* 2016;16(6):341-352.

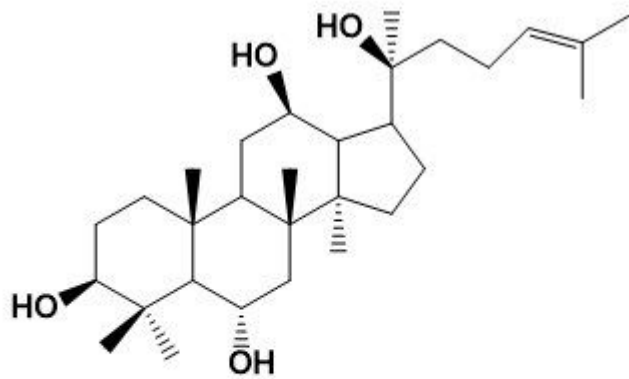
Figures



20(S)-ginsenoside CK



20(S)-protopanaxadiol (PPD)

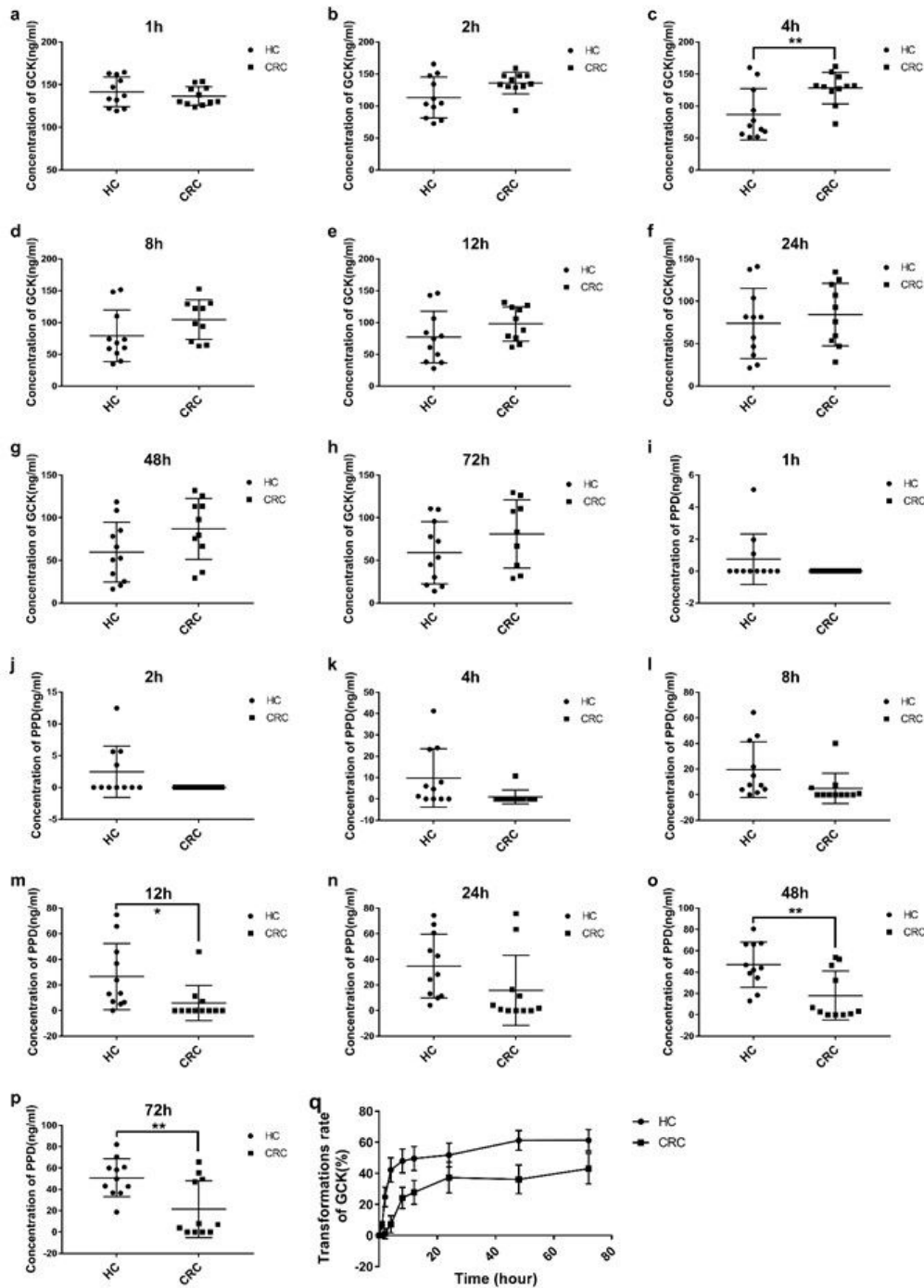


20(S)-protopanaxatriol (PPT)

Guo et al. 2020 Fig. 1

Figure 1

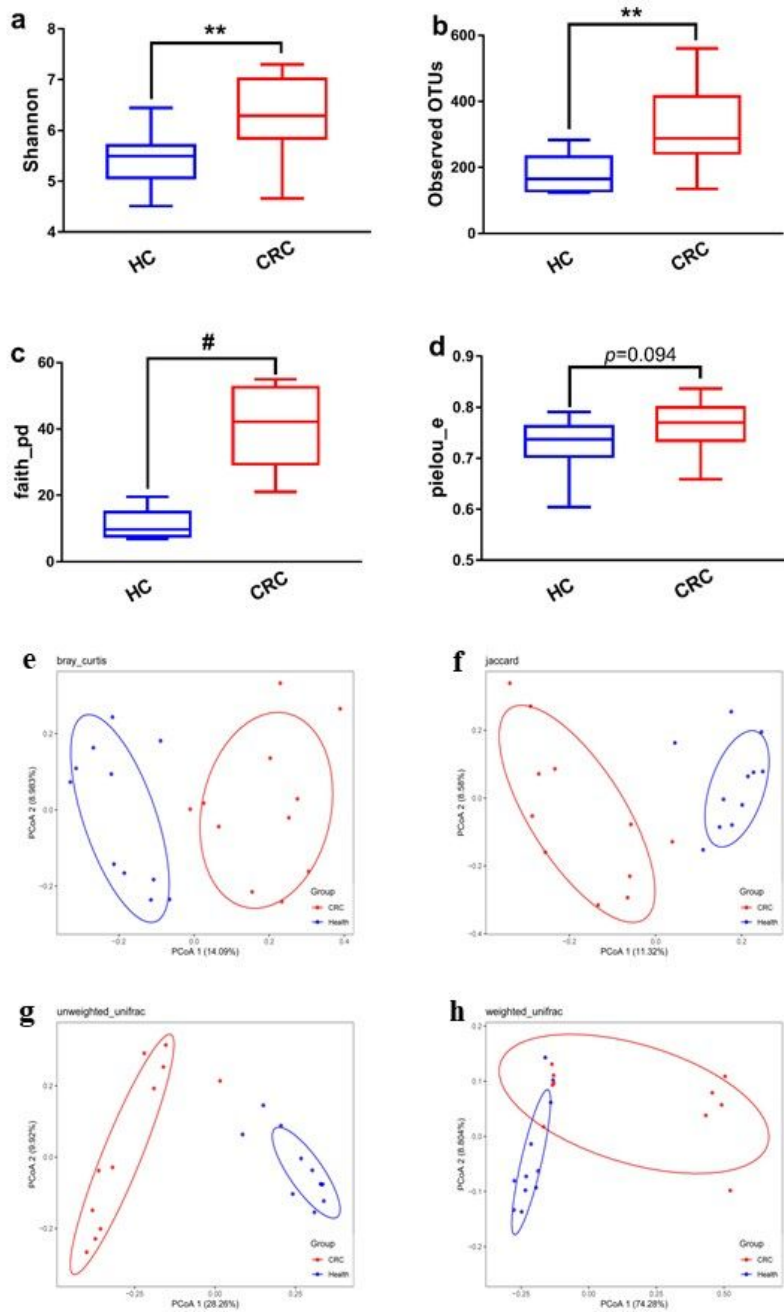
Chemical structure of GCK, PPD and PPT.



Guo et al. 2020 Fig. 2

Figure 2

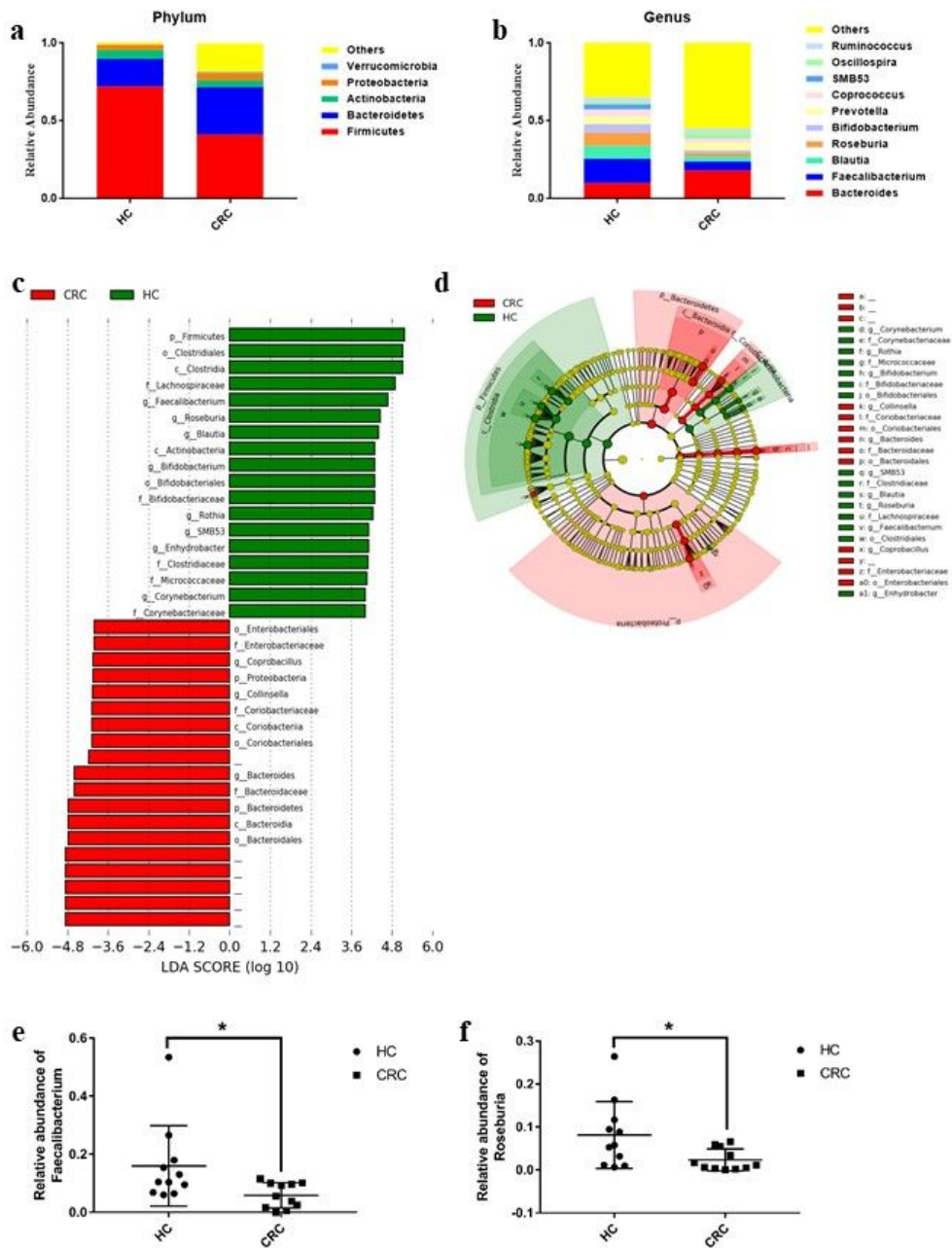
Quantitative analysis of GCK by gut microbiota. a - h: mean concentration of GCK in the incubation system among 1 - 72 h between health and CRC group; i - p: mean concentration of PPD among 1 - 72 h; q: bioconversion rate of GCK (data were expressed as mean \pm SEM); * p<0.05 and ** p<0.01; HC: health group, CRC: CRC group.



Guo et al. 2020 Fig. 3

Figure 3

Alpha diversity (a - d) and beta diversity (e - h) of gut microbiota. a: Shannon index; b: Observed OTUs; c: Faith's index; d: Pielou's index; e: Bray Curtis distance; f: Jaccard distance; g: unweighted Unifrac distance; h: weighted Unifrac distance; HC: health group, CRC: CRC group.

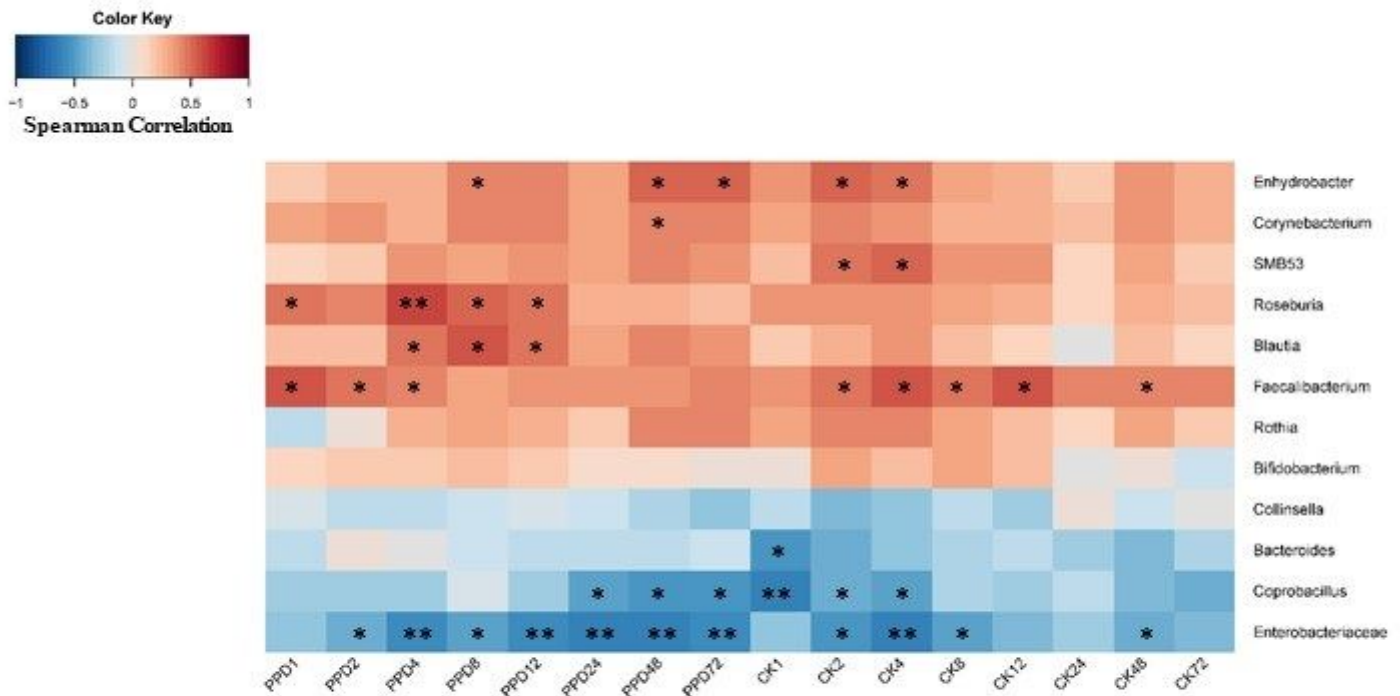


Guo et al. 2020 Fig. 4

Figure 4

Bacteria annotation in phylum level and genus level (a - b) and LefSe analysis (c - f). a: Relative abundance of top five bacteria in the phylum level between two groups; b: Relative abundance of top ten bacteria in the genus level; c: gut microbiota observed between health and CRC group ($p < 0.05$, LDA scores > 4); d: Cladogram based on LDA scores; e: Relative abundance of Faecalibacterium in each sample; f:

Relative abundance of Roseburia; significant difference of relative abundance were analyzed using Kruskal-Wallis test and Wilcoxon test; HC: health group, CRC: CRC group.



Guo et al. 2020 Fig. 5

Figure 5

Heatmap of Spearman's correlations between biotransformation of GCK and 12 differentially abundant taxon. CK 1 - 72 means bioconversion rate of GCK with 1 - 72 h incubation; PPD 1 - 72 means the concentration of PPD with 1 - 72 h incubation; * p<0.05 and ** p<0.01.

Supplementary Files

This is a list of supplementary files associated with this preprint. Click to download.

- [ChineseMedicineHWH01292021GraphicAbstract.pptx](#)
- [ChineseMedicineHWH01292021SupplementaryFigure.pptx](#)
- [ChineseMedicineHWH01292021SupplementaryTable.docx](#)